

Freeze-in bino dark matter in high-scale supersymmetry

Chengcheng Han^{1,2,†} Peiwen Wu^{3,*} Jin Min Yang^{4,5,‡} and Mengchao Zhang^{6,§}

¹*School of Physics, Sun Yat-Sen University, Guangzhou 510275, People's Republic of China*


²*Asia Pacific Center for Theoretical Physics, Pohang 37673, Korea*

³*School of Physics, Southeast University, Nanjing 211189, People's Republic of China*

⁴*CAS Key Laboratory of Theoretical Physics, Institute of Theoretical Physics, Chinese Academy of Sciences, Beijing 100190, People's Republic of China*

⁵*School of Physics, Henan Normal University, Xinxiang 453007, People's Republic of China*

⁶*Department of Physics and Siyuan Laboratory, Jinan University, Guangzhou 510632, People's Republic of China*

 (Received 4 September 2023; accepted 7 December 2023; published 9 February 2024)

We explore a scenario of high-scale supersymmetry where all supersymmetric particles except gauginos stay at a high-energy scale M_{SUSY} that is much larger than the reheating temperature T_{RH} . The dark matter is dominated by a bino component with mass around the electroweak scale and the observed relic abundance is mainly generated by the freeze-in process during the early Universe. Considering the various constraints, we identify two available scenarios in which the supersymmetric sector at an energy scale below T_{RH} consists of (a) bino or (b) bino and wino. Typically, for a bino mass around 0.1–1 TeV and a wino mass around 2 TeV, we find that M_{SUSY} should be around 10^{13-14} GeV with T_{RH} around 10^{4-6} GeV.

DOI: [10.1103/PhysRevD.109.035008](https://doi.org/10.1103/PhysRevD.109.035008)

I. INTRODUCTION

Supersymmetry (SUSY) [1–6] is a significant theoretical framework aiming at extending the Standard Model (SM), drawing inspiration from the pursuit of a quantum gravity theory, particularly within the context of superstring theory. In the field of phenomenology, SUSY not only provides a viable candidate for dark matter (DM), which plays a crucial role in the formation of large-scale structures in the Universe, but also contributes to the renormalization group running of gauge couplings through the inclusion of additional particles near the electroweak scale. This property of SUSY facilitates the potential unification of the three fundamental forces at high-energy scales. It has long been postulated that SUSY DM takes the form of weakly interacting massive particles (WIMPs) that can be probed through diverse experiments [7–17]. However, the absence of confirmed DM signals poses significant challenges to the standing of SUSY DM. The current LHC search results indicate that SUSY particles seem to be heavier than the

electroweak scale [18,19], thus challenging the WIMP paradigm of SUSY (for recent reviews on SUSY in light of current experiments, see, e.g., [20–22]).

Given the current situation, in this study we consider an alternative scenario of SUSY DM in which gauginos are located at a low-energy scale, while all other SUSY partners exist at a significantly higher scale M_{SUSY} . This scenario is a special case of the split SUSY [23–26], where Higgsinos are also taken to be a similar scale as sfermions. One should note that the Higgs sector in this scenario is fine-tuned [27–34] and it might be a consequence of the anthropic principle. However, in this work we will assume that SUSY still provides a candidate of DM and we will specifically consider the minimal supersymmetric standard model (MSSM). Since the measurement of gamma rays from the MAGIC Collaboration [35] has strongly constrained the possibility of wino DM,¹ the only viable DM candidate in the MSSM is bino. However, it is widely known that pure bino DM is typically overabundant from the freeze-out mechanism [36] due to its weak coupling with the visible sector [37,38]. Alternatively, a bino particle with a rather weak coupling may serve as a suitable candidate for feebly interacting massive particle DM with a correct relic abundance generated via the freeze-in mechanism [39], with assumptions that the reheating process solely occurs in the SM sector and the reheating temperature T_{RH} is lower than the SUSY scale M_{SUSY} .

*Corresponding author: pwwu@seu.edu.cn

†hanchch@mail.sysu.edu.cn

‡jmyang@itp.ac.cn

§mczhang@jnu.edu.cn

Published by the American Physical Society under the terms of the Creative Commons Attribution 4.0 International license. Further distribution of this work must maintain attribution to the author(s) and the published article's title, journal citation, and DOI. Funded by SCOAP³.

¹There is still viable parameter space for wino dark matter assuming the core profile of the DM.

In this work, we study the possibility that the bino DM in the MSSM is generated via the freeze-in process during the early Universe. We assume that all MSSM particles except gauginos share similar mass M_{SUSY} , which is much higher than the reheating temperature T_{RH} of the Universe. To generate enough relic abundance of bino dark matter, we always require the bino mass lower than the reheating temperature. While for the mass of winos or gluinos, it could be either higher or lower than the reheating temperature T_{RH} depending on the different scenarios we consider.

The paper is organized as follows. In Sec. II we present the model setup. In Sec. III we first overview the physics

related to dark matter and then study the dominate channels for bino freeze-in production. In Sec. IV we give the numerical results and discuss the experimental limits on the model parameter space relevant for our scenarios. We draw the conclusions in Sec. V and leave the calculation details for the Appendixes.

II. MODEL OF HEAVY SUPERSYMMETRY

Since we are considering a scenario of high-scale supersymmetry in which only gauginos are at low-energy scale, the relevant Lagrangian terms are

$$\begin{aligned} \mathcal{L} \supset & - \sum_{f=q,l} M_{\tilde{f}}^2 \tilde{f}^* \tilde{f} + \left[\left(\sum_{A=1,2,3} -\frac{1}{2} M_A \tilde{V}^{A,a} \tilde{V}^{A,a} \right) - \mu \tilde{H}_u \cdot \tilde{H}_d + b \mu H_u \cdot H_d + \text{H.c.} \right] \\ & - \sum_{A=1,2} \sqrt{2} g_A [H_u^* (T^{A,a} \tilde{V}^{A,a}) \tilde{H}_u + H_d^* (T^{A,a} \tilde{V}^{A,a}) \tilde{H}_d + \text{H.c.}] - \sum_{A=1,2,3} \sqrt{2} g_A \left[\sum_{f=q,l} \tilde{f}^* (T^{A,a} \tilde{V}^{A,a}) f + \text{H.c.} \right] \\ & - (M_{H_u}^2 + |\mu|^2) H_u^* H_u - (M_{H_d}^2 + |\mu|^2) H_d^* H_d, \end{aligned} \quad (2.1)$$

where $A = 1, 2, 3$ correspond to the SM gauge group $U(1)_Y, SU(2)_L, SU(3)_C$, respectively, and a denotes the corresponding indices in adjoint representation of group A . Fields $\tilde{V}^{A,a}, \tilde{H}_u, \tilde{H}_d$, and \tilde{f} are the superpartners of the SM vector gauge bosons $V^{A,a} = B, W^{1\sim 3}, G^{1\sim 8}$, scalar doublets H_u, H_d , and fermions f . The fields H_u, H_d, \tilde{H}_u , and \tilde{H}_d are defined as

$$\begin{aligned} H_u &= \begin{pmatrix} H_u^+ \\ H_u^0 \end{pmatrix}, & \tilde{H}_u &= \begin{pmatrix} \tilde{H}_u^+ \\ \tilde{H}_u^0 \end{pmatrix}, & H_d &= \begin{pmatrix} H_d^0 \\ H_d^- \end{pmatrix}, \\ \tilde{H}_d &= \begin{pmatrix} \tilde{H}_d^0 \\ \tilde{H}_d^- \end{pmatrix}. \end{aligned} \quad (2.2)$$

For the Higgs sector, we need a SM-like Higgs boson H_{SM} near the electroweak scale [40,41]. This is obtained from the mixing between the two Higgs doublets H_u and H_d in the MSSM,

$$\begin{aligned} H_u &= \begin{pmatrix} H_u^+ \\ H_u^0 \end{pmatrix} = \sin \beta H_{\text{SM}} + \cos \beta H_{\text{NP}} \\ &= \sin \beta \begin{pmatrix} G_{\text{SM}}^+ \\ H_{\text{SM}}^0 \end{pmatrix} + \cos \beta \begin{pmatrix} H_{\text{NP}}^+ \\ H_{\text{NP}}^0 \end{pmatrix}, \end{aligned} \quad (2.3)$$

$$\begin{aligned} (-i\sigma^2) H_d^* &= \begin{pmatrix} -(H_d^-)^* \\ (H_d^0)^* \end{pmatrix} = \cos \beta H_{\text{SM}} - \sin \beta H_{\text{NP}} \\ &= \cos \beta \begin{pmatrix} G_{\text{SM}}^+ \\ H_{\text{SM}}^0 \end{pmatrix} - \sin \beta \begin{pmatrix} H_{\text{NP}}^+ \\ H_{\text{NP}}^0 \end{pmatrix}, \end{aligned} \quad (2.4)$$

where σ^2 is the second Pauli matrix, and $\tan \beta = \langle H_u^0 \rangle / \langle H_d^0 \rangle$ with $\langle H_u^0 \rangle$ and $\langle H_d^0 \rangle$ being the vacuum expectation values (VEVs). Such mixings can be realized by properly choosing Higgs mass parameters μ, M_{H_u}, M_{H_d} , and b . The subscript NP in H_{NP} denotes the new physics (NP) Higgs doublet in the MSSM accompanying the SM one.² Since the mass parameters M_{H_u}, M_{H_d}, b , and μ are all much larger than the electroweak scale, a tuning of these parameters is needed to get a light Higgs boson at electroweak scale [27,28,30–32]. We need also match the Higgs self-coupling to be the SUSY value at the scale of M_{SUSY} ,

$$\lambda(M_{\text{SUSY}}) = \frac{g_1^2 + g_2^2}{4} \cos^2 2\beta. \quad (2.5)$$

Note that the Higgs self-coupling λ becomes very small at the high-energy scale due to the renormalization group equation running, and thus the β value should get close to $\pi/4$ and $\tan \beta \approx 1$. We will fix $\tan \beta = 1$ as the benchmark parameter throughout this work for simplicity.

Generally, when considering physical processes at temperature $T \ll M_{\text{SUSY}}$, we can integrate out the heavy mediators with mass $\mu, M_{\tilde{f}} \sim M_{\text{SUSY}} \gg T_{\text{RH}}$ and get the following effective operators at the level of dimensions five

²Note that, in order not to increase the complexity of notation, we do not further perform the expansion of the complex but electrically neutral scalars $H_{\text{SM}}^0, H_{\text{NP}}^0$ into real and imaginary parts. However, one needs to beware that $G_{\text{SM}}^{\pm}, H_{\text{SM}}^0$ contain the Goldstone boson modes to be absorbed into vector gauge bosons W^{\pm}, Z^0 after the electroweak symmetry breaking (EWSB).

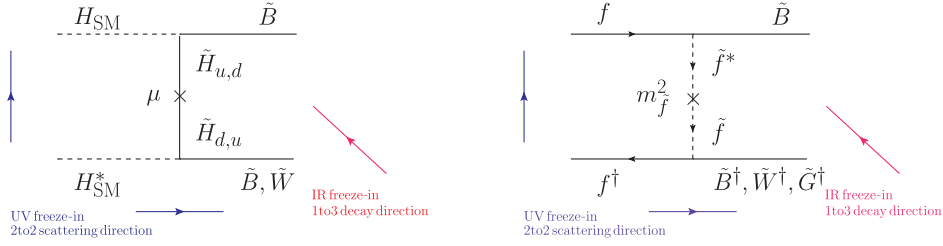


FIG. 1. Schematic plots for interactions of DM composed of pure \tilde{B} with SM after cosmological reheating considered in this work, which would induce dimension-five (left) and dimension-six (right) effective operators. The SM Higgs boson H_{SM} originates from the mixing between MSSM Higgs doublets H_u, H_d . Colored lines indicate the direction of freeze-in production when applicable. Additional Hermitian conjugated processes also exist when the amplitudes are complex. See more discussions in the main text.

and six, respectively:

$$\text{dimension 5: } \propto \frac{1}{\mu} |H_{\text{SM}}|^2 (\tilde{B} \tilde{B}, \tilde{B} \tilde{W}), \quad (2.6)$$

$$\text{dimension 6: } \propto \frac{1}{M_{\tilde{f}}^2} (f^\dagger \tilde{B}^\dagger) (f \tilde{B}, f \tilde{W}, f \tilde{G}). \quad (2.7)$$

Since we assume the mass parameters of Higgsinos μ and sfermions $M_{\tilde{f}}$ around M_{SUSY} , the dominant process would be from the dimension-five (dim-5) operators. Nevertheless we also present the processes related to dim-6 operators for completeness.

We acknowledge that a majority of the significant processes are evaluated at energy scales considerably beneath M_{SUSY} . The recommended approach entails initiating the integration procedure for the massive particle to derive the effective operators of dimension 5 and 6, along with their corresponding Wilson coefficients, within the realm of M_{SUSY} . Subsequently, the computation of these Wilson coefficients at the pertinent scale is achieved by employing the renormalization group equations to track the evolution of the operators. Notably, there exists a potential correction to the primary outcome, potentially on the order of $O(1)$, yet the fundamental framework remains robust. We leave the investigation of this effect for future study.

III. FREEZE-IN BINO DARK MATTER IN MSSM

A. Particle spectrum

Despite the existence of new Higgs bosons and many supersymmetric partners of the SM particles, the MSSM particle spectrum we consider in this work consist of two sectors distinguished by their characteristic mass scales. Although not making significant difference for the mass spectrum structure before and after EWSB, we take the pre-EWSB case as an illustration.

- (1) *Heavy sector, inactive* after cosmological reheating
 Mass: $M \sim M_{\text{SUSY}} \gg T_{\text{RH}}$
 - (a) Higgs bosons not in SM: $H_{\text{NP}}^0, A, H_{\text{NP}}^\pm$,
 - (b) sfermions \tilde{f} ,
 - (c) Higgsinos \tilde{H}_u, \tilde{H}_d .

- (2) *Light sector, active* after cosmological reheating

Mass: $M \sim \mathcal{O}(1) \text{ TeV} \ll M_{\text{SUSY}}$

- (a) SM particles,
- (b) bino \tilde{B} , consisting of cosmological DM with mass $M_1 < T_{\text{RH}}$,
- (c) winos \tilde{W} , with mass M_2 ,
- (d) gluinos \tilde{G} , with mass M_3 .

In the above we utilized gauge eigenstates for description, since \tilde{B}, \tilde{W} do not mix with Higgsinos \tilde{H}_u, \tilde{H}_d before EWSB when the SM Higgs boson H_{SM} has not acquired the VEV.

B. Bino production from freeze-in mechanism

In the early stage of the Universe before EWSB when the gaugino states \tilde{B}, \tilde{W} do not mix with Higgsinos \tilde{H}_u, \tilde{H}_d , pure \tilde{B} acting as DM can only interact with the SM via mediators with heavy mass near the scale M_{SUSY} , as shown in Fig. 1. Because of the suppressed interacting strength, the cosmological production of bino DM in our scenario proceeds via the freeze-in mechanism. In the following, we consider the contributions to bino DM production from several typical processes.³

C. Case I: Bino freeze-in from $HH^* \rightarrow \tilde{B}\tilde{B}$

This case corresponds to the left panel of Fig. 1 but without winos \tilde{W} . After integrating out the heavy Higgsinos, the relevant dim-5 effective interaction is given by (the details are given in Appendix A)

$$\mathcal{L}_{HH^* \rightarrow \tilde{B}\tilde{B}}^{\text{eff}} = \frac{2g_1^2 Y_H^2}{\mu} \sin\beta \cos\beta (|H_{\text{SM}}|^2) (\tilde{B} \tilde{B} + \tilde{B}^\dagger \tilde{B}^\dagger), \quad (3.1)$$

where $|H_{\text{SM}}|^2 = G_{\text{SM}}^+ (G_{\text{SM}}^+)^* + (H_{\text{SM}}^0) (H_{\text{SM}}^0)^*$. In the subscript $HH^* \rightarrow \tilde{B}\tilde{B}$ on the left side (and hereafter when not causing any confusion), we denote H_{SM} as H to simplify

³After electroweak phase transition occurs and H_{SM} acquires VEV, the top and bottom vertices in the left panel of Fig. 1 imply the mixing between \tilde{B}, \tilde{W} and \tilde{H}_u, \tilde{H}_d , resulting in the mass eigenstates of electrically neutral neutralinos $\tilde{\chi}_{1,2,3,4}^0$ and charged $\tilde{\chi}_{1,2}^\pm$ (see discussion in Sec. IV A).

the notation, and all fields in the initial and final states of the process should be understood in the sense of physical particles.⁴ With more details given in Appendix B, Eq. (3.1) would induce the Boltzmann equation of the bino number density,

$$\frac{d}{dt}n_{\tilde{B}} + 3\mathcal{H}n_{\tilde{B}} = \mathbf{C}_{HH^* \rightarrow \tilde{B}\tilde{B}} \approx \frac{g_1^4}{4\pi^5} \frac{\sin^2\beta \cos^2\beta}{\mu^2} T^6. \quad (3.2)$$

The above equation can be modified to a differential equation about bino yield $Y_{\tilde{B}} = n_{\tilde{B}}/S$ (S is the entropy density) and temperature T ,

$$\begin{aligned} \frac{dY_{HH^* \rightarrow \tilde{B}\tilde{B}}(T)}{dT} &= -\frac{\mathbf{C}_{HH^* \rightarrow \tilde{B}\tilde{B}}}{ST\mathcal{H}} \\ &\approx -(1.25 \times 10^{-3}) \times M_{\text{Pl}} \frac{\mathbf{C}_{HH^* \rightarrow \tilde{B}\tilde{B}}}{T^6} \\ &\approx -(1 \times 10^{-6}) \times M_{\text{Pl}} g_1^4 \frac{\sin^2\beta \cos^2\beta}{\mu^2}, \end{aligned}$$

where $M_{\text{Pl}} \approx 1.22 \times 10^{19}$ GeV is the Planck mass, $S = 2\pi^2 g_* T^3/45$, and Hubble expansion rate $\mathcal{H} \approx 1.66\sqrt{g_*} T^2/M_{\text{Pl}}$ with $g_* = 106.75$ before EWSB. Performing a simple integration from reheating temperature, it can be found that the final yield of \tilde{B} depends on the reheating temperature T_{RH} which corresponds to the ultraviolet (UV) freeze-in scenario [39,43],

$$Y_{HH^* \rightarrow \tilde{B}\tilde{B}}(\infty) \approx (1 \times 10^{-6}) \times M_{\text{Pl}} g_1^4 \frac{\sin^2\beta \cos^2\beta}{\mu^2} T_{\text{RH}}, \quad (3.3)$$

and the corresponding current relic abundance is given by

$$\begin{aligned} (\Omega_{\tilde{B}} h^2)_{HH^* \rightarrow \tilde{B}\tilde{B}} &= M_1 \frac{Y_{HH^* \rightarrow \tilde{B}\tilde{B}}(\infty) S_0}{\rho_{cr}} \\ &\approx Y_{HH^* \rightarrow \tilde{B}\tilde{B}}(\infty) \left(\frac{M_1}{\text{TeV}} \right) \times (2.72 \times 10^{11}). \end{aligned} \quad (3.4)$$

D. Case II: Fermion scattering process $f\bar{f} \rightarrow \tilde{B}\tilde{B}$

After integrating out sfermions with heavy mass $M_{\tilde{q},\tilde{l}} \sim M_{\text{SUSY}}$ in the right panel of Fig. 1, the effective interactions between the SM fermion pair and \tilde{B} pair have the following form at dimension six (for more details, see Appendix C):

$$\mathcal{L}_{f\bar{f} \rightarrow \tilde{B}\tilde{B}}^{\text{eff}} = \sum_{f=q,l} \frac{(\sqrt{2}g_1 Y_f)(\sqrt{2}g_1 Y_{\bar{f}})}{M_{\tilde{f}}^2} (f^\dagger \tilde{B}^\dagger)(f\tilde{B}), \quad (3.5)$$

⁴Discussion on the naming convention of particles, states, and fields can be found in, e.g., [42].

where, for simplicity, we consider a universal mass for all the fermions, i.e., $M_{\tilde{f}} \equiv M_{\tilde{q}} = M_{\tilde{l}}$.

Thus, the Boltzmann equation is

$$\begin{aligned} \frac{dY_{f\bar{f} \rightarrow \tilde{B}\tilde{B}}(T)}{dT} &= -\frac{\mathbf{C}_{f\bar{f} \rightarrow \tilde{B}\tilde{B}}}{ST\mathcal{H}} \\ &\approx -(1.25 \times 10^{-3}) \times M_{\text{Pl}} \frac{\mathbf{C}_{f\bar{f} \rightarrow \tilde{B}\tilde{B}}}{T^6} \\ &\approx -(8.6 \times 10^{-5}) \times M_{\text{Pl}} \frac{g_1^4}{M_{\tilde{f}}^4} T^2, \end{aligned} \quad (3.6)$$

and correspondingly,

$$Y_{f\bar{f} \rightarrow \tilde{B}\tilde{B}}(\infty) \approx (4.7 \times 10^{-7}) \times \frac{M_{\text{Pl}}}{M_{\tilde{f}}^4} T_{\text{RH}}^3, \quad (3.7)$$

$$\begin{aligned} (\Omega_{\tilde{B}} h^2)_{f\bar{f} \rightarrow \tilde{B}\tilde{B}} &= M_1 \frac{Y_{f\bar{f} \rightarrow \tilde{B}\tilde{B}}(\infty) S_0}{\rho_{cr}} \\ &\approx Y_{f\bar{f} \rightarrow \tilde{B}\tilde{B}}(\infty) \left(\frac{M_1}{\text{TeV}} \right) \times (2.72 \times 10^{11}). \end{aligned} \quad (3.8)$$

E. Case III: Gluino/wino scattering or decay processes

As indicated by blue colored arrows in Fig. 1, the $2 \rightarrow 2$ scattering processes consist of two ways of generating bino DM when combining $U(1)_Y$ with $SU(2)_L$ or $SU(3)_C$ interactions, related by the cross symmetry. Moreover, we can also have the red colored arrow indicating $1 \rightarrow 3$ ($1 \rightarrow 2$) decay processes generating binos before (after) EWSB when the cosmological temperature drops below the scale of M_2 or M_3 (equivalently, when the age of the Universe reaches the lifetime of \tilde{W} and \tilde{G}).

Similar to the previous two cases, integrating out heavy Higgsino and sfermions would generate the following dim-5 and dim-6 effective operators:

$$\begin{aligned} \mathcal{L}_{\text{case-III}}^{\text{eff}} &= \left\{ -\sum_{b=1}^3 \frac{(\sqrt{2}g_1 Y_H)(\sqrt{2}g_2)}{\mu} \sin\beta \cos\beta \left(H^* \frac{1}{2} \sigma^b H \right) (\tilde{B}\tilde{W}^b) \right. \\ &\quad + \sum_{f=u_L, d_L, e_L, \nu} \sum_{b=1}^3 \frac{(\sqrt{2}g_1 Y_f)(\sqrt{2}g_2)}{M_{\tilde{f}}^2} (f^\dagger \tilde{B}^\dagger) \left(\frac{1}{2} \sigma^b f \tilde{W}^b \right) \\ &\quad + \sum_{f=u_L, d_L, u_R^*, d_R^*} \sum_{a=1}^8 \frac{(\sqrt{2}g_1 Y_f)(\sqrt{2}g_3)}{M_{\tilde{f}}^2} (f^\dagger \tilde{B}^\dagger) \left(\frac{1}{2} \lambda^a f \tilde{G}^a \right) \left. \right\} \\ &\quad + \text{H.c.} \end{aligned} \quad (3.9)$$

Note that the index f in the second line includes only $SU(2)_L$ doublets, while the index f in the third line includes only quarks. To highlight the difference, we use index a and b to denote generators of $SU(3)_C$ and $SU(2)_L$

interactions, respectively. Correspondingly, λ^a and σ^b are Gell-Mann and Pauli matrices, respectively.

In the following, we consider the contributions to the bino DM production from $2 \rightarrow 2$ scattering and $1 \rightarrow 3$ decay separately, while leaving the effects of $1 \rightarrow 2$ decay appearing after EWSB to Sec. IV A.

1. Case III A: $2 \rightarrow 2$ scattering involving gluinos/winos

With more details given in Appendix D, the collision terms in the Boltzmann equation for dim-5 and dim-6 operators are approximated as (ignoring the masses of all external particles)

$$\begin{aligned} \mathbf{C}_{\text{dim-5}} &= \frac{T}{2048\pi^6} \int_{4M_1^2}^{\infty} ds (s - 4M_1^2)^{1/2} K_1(\sqrt{s}/T) \\ &\quad \times \sum_{\text{internal d.o.f.}} \int d\Omega \left(|\mathcal{M}|_{HH^* \rightarrow \tilde{B}\tilde{B}}^2 + |\mathcal{M}|_{HH^* \rightarrow \tilde{B}\tilde{W}}^2 \right. \\ &\quad \left. + N_{\text{conj}} |\mathcal{M}|_{\tilde{W}H \rightarrow \tilde{B}H}^2 \right) \\ &= \left(\frac{1}{4}g_1^4 + \frac{3}{2}g_1^2g_2^2 \right) \frac{1}{\pi^5} \frac{\sin^2\beta \cos^2\beta}{\mu^2} T^6, \end{aligned} \quad (3.10)$$

$$\begin{aligned} \mathbf{C}_{\text{dim-6}} &= \frac{T}{2048\pi^6} \int_{4M_1^2}^{\infty} ds (s - 4M_1^2)^{1/2} K_1(\sqrt{s}/T) \\ &\quad \times \sum_{\text{internal d.o.f.}} \int d\Omega \left(|\mathcal{M}|_{f\bar{f} \rightarrow \tilde{B}\tilde{B}}^2 + |\mathcal{M}|_{f\bar{f} \rightarrow \tilde{B}\tilde{W}}^2 \right. \\ &\quad \left. + N_{\text{conj}} |\mathcal{M}|_{\tilde{W}f \rightarrow \tilde{B}f}^2 + |\mathcal{M}|_{f\bar{f} \rightarrow \tilde{B}\tilde{G}}^2 + N_{\text{conj}} |\mathcal{M}|_{\tilde{G}f \rightarrow \tilde{B}f}^2 \right) \\ &= \left(\frac{190}{9}g_1^4 + 30g_1^2g_2^2 + \frac{440}{3}g_1^2g_3^2 \right) \frac{1}{\pi^5} \frac{1}{M_{\tilde{f}}^4} T^8, \end{aligned} \quad (3.11)$$

where $N_{\text{conj}} = 2$ denotes the effects of the conjugated process.

2. Case III B: Decay of gluinos/winos

Following the method in [39], with $f_{\tilde{G}}$ and $f_{\tilde{W}}$ approximated by $e^{-E_{\tilde{G}}/T}$ and $e^{-E_{\tilde{W}}/T}$, the Boltzmann equation of freeze-in production for the $1 \rightarrow 3$ decay processes is

$$\begin{aligned} \frac{d}{dt} n_{\tilde{B}} + 3\mathcal{H}n_{\tilde{B}} &= \mathbf{C} \\ &\approx \frac{g_{\tilde{G}}M_3^2}{2\pi^2} TK_1\left(\frac{M_3}{T}\right) \Gamma_{\tilde{G} \rightarrow f\bar{f}\tilde{B}} + \frac{g_{\tilde{W}}M_2^2}{2\pi^2} TK_1 \\ &\quad \times \left(\frac{M_2}{T}\right) (\Gamma_{\tilde{W} \rightarrow f\bar{f}\tilde{B}} + \Gamma_{\tilde{W} \rightarrow HH^*\tilde{B}}), \end{aligned} \quad (3.12)$$

where $g_{\tilde{G}} = 16$ and $g_{\tilde{W}} = 6$ are the internal degrees of freedom (d.o.f.) of \tilde{G} and \tilde{W} , respectively. The expressions of decay width involved in the above results are listed

in Appendix E. Changing variables to yield $Y_{\tilde{B}}$ and temperature T , we then integrate over temperature evolution to obtain the final yield. If reheating temperature T_{RH} is much larger than M_2 and M_3 , then the final yield from $1 \rightarrow 3$ decay can be approximated by

$$\begin{aligned} Y_{\tilde{B}}^{1 \rightarrow 3}(\infty) &\approx \int_{T_{\text{min}}}^{T_{\text{RH}}} \frac{\mathbf{C}}{ST\mathcal{H}} dT \\ &\approx (3 \times 10^{-4}) \times M_{\text{Pl}} \left(\frac{1}{M_3^2} g_{\tilde{G}} \Gamma_{\tilde{G} \rightarrow f\bar{f}\tilde{B}} \right. \\ &\quad \left. + \frac{1}{M_2^2} g_{\tilde{W}} \Gamma_{\tilde{W} \rightarrow f\bar{f}\tilde{B}} + \frac{1}{M_2^2} g_{\tilde{W}} \Gamma_{\tilde{W} \rightarrow HH^*\tilde{B}} \right). \end{aligned} \quad (3.13)$$

It is worth pointing out that the above result is not sensitive to T_{RH} . Taking a low reheating temperature $T_{\text{RH}} = 1.1M_3$ as an example, increasing the value of T_{RH} does not modify the result significantly.

In addition to the $1 \rightarrow 3$ decay, we should also note that wino \tilde{W} with mass $M_2 < T_{\text{RH}}$ stays in the thermal bath until reaching its freeze-out moment, yielding a relic wino number density, which would later convert to the equal amount of bino number density $n_{\tilde{B}}$ via $1 \rightarrow 2$ decay $\tilde{W} \rightarrow \tilde{B} + h$ after EWSB occurs. Depending on the bino mass M_1 , this freeze-out component would also contribute to the total bino DM abundance in today's epoch. We checked that with wino mass $M_2 = 2$ TeV, the $1 \rightarrow 2$ decay contribution of $Y_{\tilde{B}}^{1 \rightarrow 2}$ to final bino yield is around 25% (1%) on the percentage level for $M_1 = 1$ (0.1) TeV [44], thus not affecting the freeze-in domination scenario of this work. We properly include the wino freeze-out contribution in our results. There is also contribution from gluino late time decay. However, to avoid the constraints from big bang nucleosynthesis (BBN), we have to set the gluino mass higher than the T_{RH} ; thus we do not include its contribution here.

IV. NUMERICAL RESULTS AND DISCUSSIONS

In Fig. 2 we show the required scales of μ ($M_{\tilde{f}}$) for dim-5 (6) operators with various T_{RH} to produce the observed bino DM relic abundance. The upper (lower) two lines correspond to dim-5 (6) operators. We can see that, due to more suppression of dim-6 operators, the needed $M_{\tilde{f}}$ are generally $\mathcal{O}(10^{-4})$ smaller than μ in the dim-5 case. If we assume $\mathcal{O}(\mu) \approx \mathcal{O}(M_{\tilde{f}})$, in order not to overclose the Universe, the dim-6 contributions would be completely negligible.

From Fig. 2, we can see that, for the case $M_{\tilde{B}} < T_{\text{RH}} \ll M_{\tilde{W}}$, the dominant production of bino dark matter is from the process $HH^* \rightarrow \tilde{B}\tilde{B}$ from the dim-5 operator. Generally, M_{SUSY} should be around 10^{13-14} GeV for $T_{\text{RH}} < 10^6$ GeV. Since the final relic abundance is

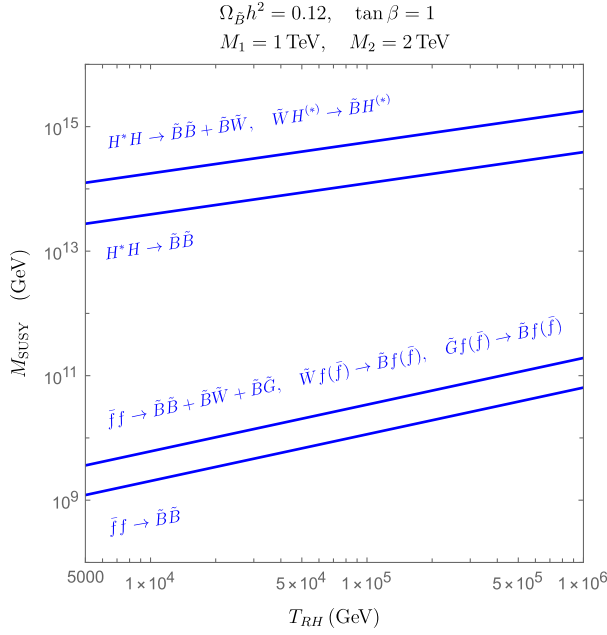


FIG. 2. Values of μ and $M_{\tilde{f}}$ to produce the observed DM abundance via the UV freeze-in processes. See more discussions in the main text.

proportional to T_{RH}/μ^2 , the M_{SUSY} could continue increasing if the reheating temperature T_{RH} becomes higher. Note that this is similar to the model of Higgs portal to fermion dark matter which is studied in [45], with which we find our results are consistent. We emphasize that our model is motivated by a more complete framework and [45] falls into one of cases we consider. Moreover, for the case $M_{\tilde{B}}, M_{\tilde{W}} < T_{\text{RH}}$, we find the wino-included process can largely enhance the annihilation rate and a higher scale is needed to satisfy the relic abundance. In this case, M_{SUSY} should be around 10^{14-15} GeV for $T_{\text{RH}} < 10^6$ GeV.

Notice that, if the gluino is in thermal equilibrium with the SM in the early Universe and the sfermions mediating the gluino decay are heavier than 10^9 GeV, the lifetime of the gluino could be longer than the age of the Universe when the BBN happens, leading to energy injection into the cosmic plasma and altering the BBN profile. In all cases considered in this work, we find M_{SUSY} is much larger than 10^9 GeV; therefore, we always need $M_{\tilde{G}} \gg T_{\text{RH}}$ to avoid the limit from BBN [46]. More discussions on BBN limits are given in Sec. IV A.

In Fig. 3 we show the comparison of final contributions and intermediate profile of UV and IR freeze-in processes to the bino DM relic abundance. It can be clearly seen that the IR freeze-in final yields from wino three-body decays are negligible compared to that of UV freeze-in processes generated by $2 \rightarrow 2$ annihilation. Moreover, the critical production moment determining the final yield of UV freeze-in locates in a much smaller x (and thus much higher temperature) than the IR freeze-in case.

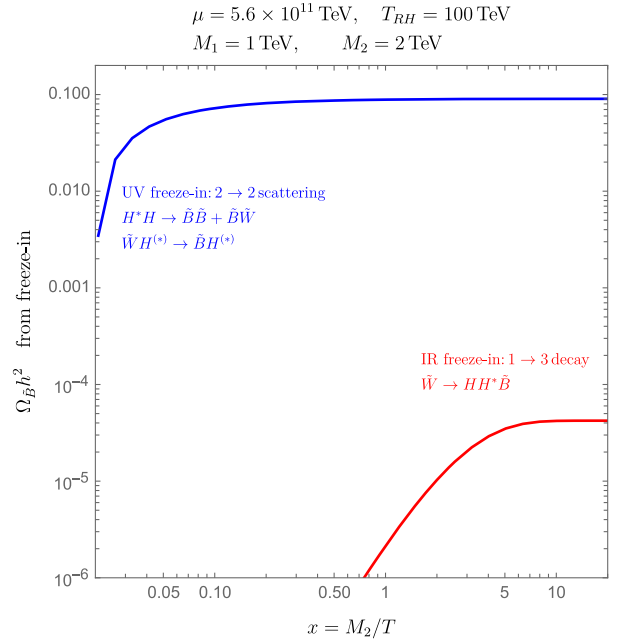


FIG. 3. Comparison between UV freeze-in and IR freeze-in. Note the difference between temperatures indicated by $x = M_2/T$ producing the correct relic density of bino DM.

A. Limits from BBN

After EWSB, the SM-like Higgs doublet needs to be replaced by

$$H = \begin{pmatrix} G^+ \\ \frac{1}{\sqrt{2}}(v + h + iG^0) \end{pmatrix}, \quad (4.1)$$

where h is the observed SM-like Higgs⁵ scalar and $v = 246$ GeV is the VEV of h . G^\pm [$G^- = (G^+)^*$] and G^0 are Goldstone bosons that form the longitudinal modes of SM gauge bosons W^\pm and Z . As mentioned earlier, the SM-like Higgs VEV will generate mixings among the gauge states $\tilde{B}, \tilde{W}, \tilde{H}_u$, and \tilde{H}_d and form mass eigenstates of charge-neutral neutralinos $\tilde{\chi}_{1,2,3,4}$ and charged charginos $\tilde{\chi}_{1,2}^\pm$ (with ascending mass order inside sectors of neutralinos and charginos, respectively). For the scenario considered in this work, the component of neutralino $\tilde{\chi}_1^0$ ($\tilde{\chi}_2^0$) is dominated by bino \tilde{B} (wino \tilde{W}^3), and the component of chargino $\tilde{\chi}_1^\pm$ is dominated by winos $\frac{1}{\sqrt{2}}(\tilde{W}^1 \mp i\tilde{W}^2)$. More details of the approximated masses and couplings can be found in [47–49]. In the following, we would utilize the language of gauge states (bino \tilde{B} , wino \tilde{W} , Higgsinos \tilde{H}_u, \tilde{H}_d) and mass eigenstates (neutralino $\tilde{\chi}^0$, chargino $\tilde{\chi}^\pm$) interchangeably before and after EWSB.

⁵If wino decays much later than electroweak phase transition, then $v = 246$ GeV is a good approximation.

Now we study the limit of BBN on our scenario from lifetimes of neutralinos and charginos. In our scenario, only neutralino $\tilde{\chi}_1^0 \approx \tilde{B}, \tilde{\chi}_2^0 \approx \tilde{W}^3$ and chargino $\tilde{\chi}_1^\pm \approx \frac{1}{\sqrt{2}}(\tilde{W}^1 \mp i\tilde{W}^2)$ existed in the primordial thermal bath. Because of the loop-induced mass splitting between $\tilde{\chi}_1^\pm$ and $\tilde{\chi}_2^0$, chargino $\tilde{\chi}_1^\pm$ can have the two-body decay $\tilde{\chi}_1^\pm \rightarrow \tilde{\chi}_2^0 \pi^\pm$ [50–53]. It makes the lifetime of $\tilde{\chi}_1^\pm$ much shorter than 1 sec, and thus it does not affect the BBN profile. However, we need to scrutinize the lifetime of $\tilde{\chi}_2^0$ more carefully. If $\tilde{\chi}_2^0$ decays after the onset of BBN, then the highly energetic decay products will cause the photodissociation or hadrodissociation and thus change the final abundances of light elements. So a bound from BBN can be put on the model parameters, especially on the SUSY scale M_{SUSY} [54,55].

It is easy to see that Fig. 1 implies the two-body decay mode of $\tilde{\chi}_2^0 \rightarrow \tilde{\chi}_1^0 h$ at the level of dim-5 after EWSB, in which case we will have

$$\begin{aligned} \mathcal{L}_{\text{eff}} &= - \sum_{b=1}^3 \frac{(\sqrt{2}g_1 Y_H)(\sqrt{2}g_2)}{\mu} \sin\beta \cos\beta \left(H^* \frac{1}{2} \sigma^b H \right) \\ &\quad \times (\tilde{B}\tilde{W}^b) + \text{H.c.} \\ &= - \frac{g_1 g_2 v}{2\mu} \sin\beta \cos\beta (G^\mp \tilde{W}^\pm \tilde{B} - h\tilde{W}^0 \tilde{B} + \text{H.c.}) \\ &\approx - \frac{g_1 g_2 v}{2\mu} \sin\beta \cos\beta (G^\mp \tilde{\chi}_1^\pm \tilde{\chi}_1^0 - h\tilde{\chi}_2^0 \tilde{\chi}_1^0 + \text{H.c.}), \end{aligned} \quad (4.2)$$

where the first term containing Goldstone boson G^\mp can be understood in the context of the Goldstone equivalence theorem (GET) for $\tilde{\chi}_1^\pm \rightarrow \tilde{\chi}_1^0 W^\pm$. It should be noticed that Eq. (4.2) does not contain the three-particle coupling $G^0 \tilde{W} \tilde{B}$ and thus would not provide a way of inferring the two-body decay mode $\tilde{\chi}_2^0 \rightarrow \tilde{\chi}_1^0 Z$ via the GET. In fact, $\tilde{\chi}_2^0 \rightarrow \tilde{\chi}_1^0 Z$ comes from the gauge covariant kinetic terms of gauginos and Higgsinos combined with gaugino mixings after EWSB. However, the decay width of $\tilde{\chi}_2^0 \rightarrow \tilde{\chi}_1^0 Z$ suffers from an extra suppression of $\frac{1}{\mu^2}$ embedded in the mass mixings compared to $\tilde{\chi}_2^0 \rightarrow \tilde{\chi}_1^0 h$ and thus can be ignored [56]. Therefore, we have the following dominant two-body decay (see Appendix F for more details):

$$\begin{aligned} \Gamma_{\tilde{\chi}_2^0 \rightarrow \tilde{\chi}_1^0 h} &\approx M_2 \frac{1}{16\pi} \left(\frac{v}{\mu} g_1 g_2 \sin\beta \cos\beta \right)^2 \left(1 - \frac{M_1^2}{M_2^2} \right) \\ &\quad \times \left(1 + \frac{M_1^2}{M_2^2} \right)^2. \end{aligned} \quad (4.3)$$

Using the GET we would obtain the same results for $\Gamma_{\tilde{\chi}_1^\pm \rightarrow \tilde{\chi}_1^0 W^\pm}$ when neglecting the gauge boson masses.

In this work, we apply the limit of BBN to the requirement that the lifetime of $\tilde{\chi}_2^0$ must be less than 0.3 sec [39]. In Fig. 4, we show the interplay between BBN constraints and freeze-in production, where the region below the black

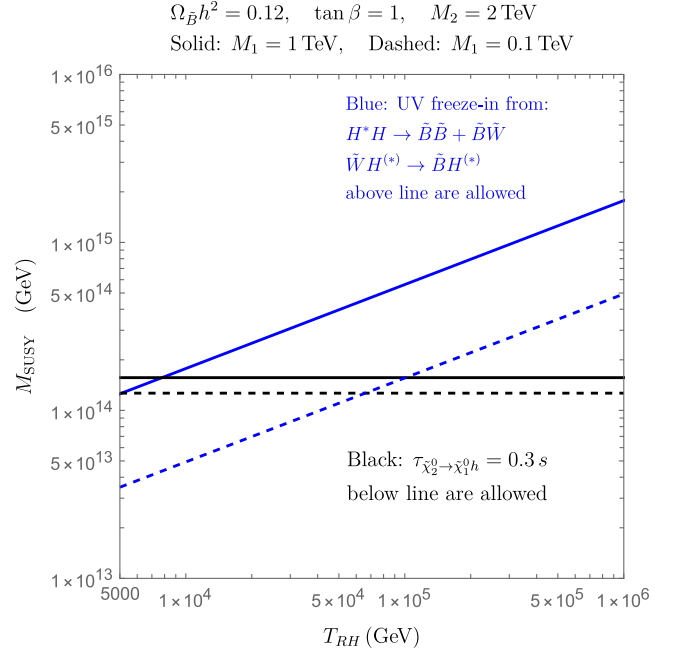


FIG. 4. Interplay between BBN constraints and freeze-in production, where the region below black lines is allowed and the region above blue lines is allowed.

lines is allowed and the region above the blue lines is allowed. We can see that, for bino mass around 0.1–1 TeV, an upper bound of $M_{\text{SUSY}} \sim 10^{14}$ TeV is needed to satisfy both phenomenological requirements.

B. Limits from direct/indirect detection

Our scenario can easily escape from the current limits of direct and indirect detection. In the case of direct detection, Eq. (3.1) after EWSB would generate the t -channel scattering of $\tilde{\chi}_1^0$ with quarks and gluons in SM nucleons mediated by SM Higgs boson, of which the event rate is suppressed by $1/\mu^2$ and is thus negligibly small. In the case of indirect detection, which is basically the inverse process of the freeze-in DM production, cosmic rays would be generated via DM pair annihilations $\tilde{\chi}_1^0 \tilde{\chi}_1^0 \rightarrow h^* \rightarrow \text{SM}$ and $\tilde{\chi}_1^0 \tilde{\chi}_1^0 \rightarrow hh \rightarrow \text{SM}$, of which the flux is again suppressed by $1/\mu^2$ and is thus not violating the current experimental bounds.

C. Limits from the LHC

The collider signals of our scenario mainly come from $pp \rightarrow \tilde{\chi}_1^\pm \tilde{\chi}_1^\mp, \tilde{\chi}_1^\pm \tilde{\chi}_2^0$ followed by $\tilde{\chi}_1^\pm \rightarrow \tilde{\chi}_2^0 \pi^\pm$ and $\tilde{\chi}_2^0 \rightarrow \tilde{\chi}_1^0 h$, which both generate the long-lived particle (LLP) signals. The LLP signatures manifest as disappearing tracks for $\tilde{\chi}_1^\pm \rightarrow \tilde{\chi}_2^0 \pi^\pm$ and displaced vertices for $\tilde{\chi}_2^0 \rightarrow \tilde{\chi}_1^0 h$, respectively. However, $\tau_{\tilde{\chi}_2^0 \rightarrow \tilde{\chi}_1^0 h} > \mathcal{O}(10^{-2})$ s would make $\tilde{\chi}_2^0$ traverse through the whole detector before decaying, without leaving any energy deposit in the calorimeters, thus

easily evading the current ATLAS [57] and CMS [58] searches for displaced vertex signals at $\sqrt{s} = 13$ TeV. As for the disappearing track signature of $\tilde{\chi}_1^\pm \rightarrow \tilde{\chi}_2^0 \pi^\pm$, ATLAS [59] and CMS [60] also performed dedicated searches using a dataset at $\sqrt{s} = 13$ TeV and imply that $\tilde{\chi}_1^\pm, \tilde{\chi}_2^0$ should be heavier than 500–600 GeV; therefore, our benchmark points with $M_2 = 2$ TeV are still available.

D. Discussions

Before ending this section, we discuss some details concerning the SUSY mass spectrum.

First, our findings indicate that, to achieve the correct dark matter relic abundance through the UV freeze-in mechanism, the typical mass scales of SUSY particles (excluding gauginos) should be in the range of 10^{13-14} GeV. An intriguing question arises concerning whether the SM Higgs boson with mass around 125 GeV can be accommodated within this framework. In heavy SUSY scenarios, as discussed in [28,31], sparticle masses around 10^{13} GeV are still viable, particularly when considering $\tan\beta = 1$ and allowing for the uncertainty in SM parameters within 1σ range. Expanding the range of uncertainty in SM parameters, particularly the top Yukawa coupling, to 2σ range allows for a significant upward adjustment of the SUSY mass scale. Notably, the work of [32] delves into high-scale SUSY within 3σ uncertainty for Standard Model parameters, with findings indicating that for $\tan\beta = 1$ a SUSY scale as high as 10^{16} GeV remains consistent with the observed SM Higgs mass. This underscores the importance of considering a reasonable range of uncertainty in SM parameters when assessing SUSY scenarios. However, it is crucial to note that future precision measurements of SM parameters hold the potential to rigorously scrutinize SUSY scenarios. Therefore, our model stands poised for being tested against these precise measurements, providing an avenue for further validation and refinement.

Second, in our study we adopted the assumption of a gluino mass greater than the reheating temperature T_{RH} to avoid potential conflict with BBN constraints. Concurrently, we presented typical mass ranges for the bino (and wino) falling within the span of 0.1–1 TeV, with T_{RH} estimated at around 10^4 – 10^6 GeV. This naturally entails the requirement for a substantial hierarchy between the gluino mass and the bino (as well as the wino) mass. Achieving such a hierarchy within the domain of supersymmetry calls for a meticulous consideration of the scenarios associated with SUSY breaking and mediation. One plausible avenue involves postulating nonuniversal gaugino masses. This can be accomplished by ascribing distinct representations to the SUSY breaking superfield Φ with nonvanishing F-terms (see, e.g., [61–63]). While the above framework provides a well-recognized means of introducing a phenomenologically oriented hierarchy among gaugino masses, attaining the desired mass ratio

between the gluino and the bino/wino may necessitate a fine-tuning of the contributions arising from these different representations.

It is crucial to emphasize that our present research predominantly focuses on delving into the phenomenological aspects, especially within the realm of dark matter. Acknowledging that a comprehensive model incorporating precise calculations of the Higgs mass and the requisite mass hierarchy for gauginos is undoubtedly imperative, we intend to actively explore the feasibility of incorporating these elements in our future work.

V. CONCLUSION

We studied a scenario of dark matter generated from the UV freeze-in mechanism, realized in the framework of the high-scale MSSM. The bino is the dark matter candidate and its relic abundance is generated by the freeze-in processes via the dim-5 or dim-6 operators. We found that the SUSY scale M_{SUSY} should be around 10^{13-15} GeV for reheating temperature in the range of 10^{4-6} GeV. We also illustrated the interplay between BBN constraints from neutral wino decay and the experimentally observed dark matter relic abundance, implying an upper bound of M_{SUSY} around 10^{14} GeV for wino mass around 2 TeV and bino mass of 0.1–1 TeV.

ACKNOWLEDGMENTS

This work was supported by the Natural Science Foundation of China (NSFC) under Grant No. 12105118, No. 11947118, No. 12075300, No. 11821505, and No. 12335005, the Peng-Huan-Wu Theoretical Physics Innovation Center (12047503), the CAS Center for Excellence in Particle Physics (CCEPP), and the Key Research Program of the Chinese Academy of Sciences under Grant No. XDPB15. C.H. acknowledges support from the Sun Yat-Sen University Science Foundation and the Fundamental Research Funds for the Central Universities, Sun Yat-sen University under Grant No. 23qnp58. P.W. acknowledges support from Natural Science Foundation of Jiangsu Province (Grant No. BK20210201), Fundamental Research Funds for the Central Universities, Excellent Scholar Project of Southeast University (Class A), and the Big Data Computing Center of Southeast University.

APPENDIX A: NOTATION CONVENTIONS AND DIM-5 OPERATOR IN CASE I

In Eq. (2.1), the dot product means $\tilde{H}_u \cdot \tilde{H}_d = \tilde{H}_{u,i}(i\sigma^2)^{ij}\tilde{H}_{d,j} = \tilde{H}_u^+\tilde{H}_d^- - \tilde{H}_u^0\tilde{H}_d^0$ to realize the isospin symmetry $SU(2)_L$ where σ^2 is the second Pauli matrix. The Kronecker delta function δ_i^j manifests the $SU(2)_L$ blindness of the $U(1)_Y$ interactions under consideration for bino production and $Y_{H_u} = +1/2, Y_{H_d} = -1/2$ are the

hypercharges of doublets H_u, H_d , respectively. We follow the convention of [42] and impose the left-chiral two-component spinor formalism for Higgsinos $\tilde{H}_u^+, \tilde{H}_u^0, \tilde{H}_d^0, \tilde{H}_d^-$ and bino \tilde{B} (as well as winos \tilde{W} and gluinos \tilde{g} in later discussion). For case I in Sec. III B, the relevant Lagrangian terms are

$$\begin{aligned} \mathcal{L} \supset & -\frac{1}{2} M_1 \tilde{B} \tilde{B} - \mu (\tilde{H}_u^+ \tilde{H}_d^- - \tilde{H}_u^0 \tilde{H}_d^0) + \text{H.c.} \\ & - \frac{g_1}{\sqrt{2}} (H_u^+)^* \tilde{H}_u^+ \tilde{B} - \frac{g_1}{\sqrt{2}} (H_u^0)^* \tilde{H}_u^0 \tilde{B} + \frac{g_1}{\sqrt{2}} (H_d^-)^* \tilde{H}_d^- \tilde{B} \\ & + \frac{g_1}{\sqrt{2}} (H_d^0)^* \tilde{H}_d^0 \tilde{B} + \text{H.c.} \end{aligned} \quad (\text{A1})$$

After integrating out Higgsinos with mass μ , we obtain the dim-5 operator between SM Higgs boson H_{SM} and \tilde{B} DM,

$$\begin{aligned} \mathcal{L}_{HH^* \rightarrow \tilde{B}\tilde{B}}^{\text{eff}} &= -\frac{(\sqrt{2}g_1 Y_H)(\sqrt{2}g_1 Y_H)}{\mu} (H_u^* \cdot H_d^*) \tilde{B} \tilde{B} + \text{H.c.} \\ &= -\frac{2g_1^2 Y_H^2}{\mu} \sin\beta \cos\beta (H_{\text{SM}}^* \cdot i\sigma^2 H_{\text{SM}}) (\tilde{B} \tilde{B} + \tilde{B}^\dagger \tilde{B}^\dagger) \\ &= \frac{2g_1^2 Y_H^2}{\mu} \sin\beta \cos\beta (|H_{\text{SM}}|^2) (\tilde{B} \tilde{B} + \tilde{B}^\dagger \tilde{B}^\dagger), \end{aligned} \quad (\text{A2})$$

where $Y_H = |Y_{H_u}| = |Y_{H_d}| = 1/2$ and the dot products are $H_u^* \cdot H_d^* = (H_u^+)^* (H_d^-)^* - (H_u^0)^* (H_d^0)^*$.

APPENDIX B: BOLTZMANN EQUATION AND CALCULATION DETAILS OF FREEZE-IN DM IN CASE I

In the homogeneous and isotropic Universe, the production of binos is described by the following Boltzmann equation [36]:

$$\frac{d}{dt} n_{\tilde{B}} + 3\mathcal{H} n_{\tilde{B}} = \mathbf{C}, \quad (\text{B1})$$

with $n_{\tilde{B}}$ denoting the number density of the bino particle, and \mathcal{H} is the Hubble expansion rate. Taking $HH^* \rightarrow \tilde{B}\tilde{B}$ (\tilde{B} means the physical bino particle) in case I of Sec. III B as an example, we have [64]

$$\begin{aligned} \mathbf{C}_{ij \rightarrow kl} &= N \times \frac{1}{S} \times \left\{ \int \frac{d^3 p_i}{(2\pi)^3 2E_i} \frac{d^3 p_j}{(2\pi)^3 2E_j} \frac{d^3 p_k}{(2\pi)^3 2E_k} \right. \\ &\quad \times \frac{d^3 p_l}{(2\pi)^3 2E_l} (2\pi)^4 \delta^4(p_i + p_j - p_k - p_l) \\ &\quad \times [f_i f_j (1 - f_k)(1 - f_l) - f_k f_l (1 + f_i)(1 + f_j)] \\ &\quad \left. \times \sum_{\text{internal d.o.f.}} |\mathcal{M}_{ij \rightarrow kl}^2| \right\}, \end{aligned} \quad (\text{B2})$$

where $f_{i,j,k,l}$ are the phase space distribution functions. The number density, taking f_i as example, is defined as

$$n_i \equiv g_i \int \frac{d^3 p}{(2\pi)^3} f_i(p), \quad (\text{B3})$$

in which g_i is the internal d.o.f. of particle i . The factor N denotes the number of particles under consideration produced in the final state and the factor $1/S$ originates from the phase space suppression due to the *identical* particles in the initial and final states. For $HH^* \rightarrow \tilde{B}\tilde{B}$ we have $N = 2$ and $1/S = 1/(N!) = 1/2$. After some manipulations and neglecting the negligible backward process, we have [64]

$$\mathbf{C}_{ij \rightarrow kl} \approx \frac{T}{32\pi^4} \int_{(m_k+m_l)^2}^{\infty} ds p_{ij} W_{ij \rightarrow kl} K_1(\sqrt{s}/T), \quad (\text{B4})$$

$$W_{ij \rightarrow kl} = \frac{p_{kl}}{16\pi^2 \sqrt{s}} \sum_{\text{internal d.o.f.}} \int d\Omega |\mathcal{M}_{ij \rightarrow kl}^2|, \quad (\text{B5})$$

$$p_{ij} = \frac{\sqrt{s - (m_i + m_j)^2} \sqrt{s - (m_i - m_j)^2}}{2\sqrt{s}}, \quad (\text{B6})$$

where p_{kl} is similar to p_{ij} . After summing over all bino spin states s_1, s_2 and isospin states of the SM-like Higgs boson, we have the amplitude square (s is the square of the central energy),

$$\begin{aligned} &\sum_{\text{internal d.o.f.}} \int d\Omega |\mathcal{M}_{HH^* \rightarrow \tilde{B}\tilde{B}}^2|, \\ &\approx (2\pi) \times \left[\sum_{i,j=1}^2 (\delta_i^j)^2 \right] [Y_H^4] \left(\frac{g_1 g_2 \sin\beta \cos\beta}{\mu} \right)^2 \\ &\quad \times \left[64s \left(1 - \frac{4M_1^2}{s} \right)^{\frac{3}{2}} \right] \\ &\approx (16\pi) \times \frac{g_1^4}{\mu^2} \sin^2\beta \cos^2\beta s. \end{aligned} \quad (\text{B7})$$

We modify the MSSM file available in FeynRules [65,66] to highlight the gauge state interactions and then export to FeynArts [67] augmented with FeynCalc [68] to perform the calculation.

Since we are considering freeze-in production of \tilde{B} , $f_{1,2}$ in Eq. (B2) can be ignored. We can further approximate $f_{3,4}$ by Maxwell-Boltzmann distribution, i.e., $f_{3,4} \approx e^{-E_{3,4}/T}$. Then the collision term can be rewritten as [43,64,69]

$$\begin{aligned}
C_{HH^* \rightarrow \tilde{B} \tilde{B}} &\approx \frac{T}{2048\pi^6} \int_{4M_1^2}^{\infty} ds (s - 4M_1^2)^{1/2} K_1(\sqrt{s}/T) \\
&\times \sum_{\text{internal d.o.f.}} \int d\Omega |\mathcal{M}|_{HH^* \rightarrow \tilde{B} \tilde{B}}^2, \\
&\approx \frac{T}{128\pi^5} \frac{g_1^4 \sin^2 \beta \cos^2 \beta}{\mu^2} \int_{4M_1^2}^{\infty} ds s^{3/2} K_1(\sqrt{s}/T).
\end{aligned} \tag{B8}$$

Here K_1 is the Bessel function of the second kind, and we treat the SM-like Higgs boson in the initial state as being massless. In the case where $M_1 \ll T$, the collision term can be approximated as [using $\int_0^\infty dx x^4 K_1(x) = 16$]

$$\begin{aligned}
\int_{4M_1^2}^{\infty} ds s^{3/2} K_1(\sqrt{s}/T) &\approx \int_0^\infty (dxT)(2xT)(xT)^3 K_1(x) \\
&= 2T^5 \int_0^\infty dx x^4 K_1(x) = 32T^5.
\end{aligned} \tag{B9}$$

APPENDIX C: THE CALCULATION DETAILS IN CASE II

We use $f = q, l$ with $q = u_L, d_L, u_R^\dagger, d_R^\dagger$ and $l = \nu, e_L, e_R^\dagger$ to denote the left-handed two-component Weyl spinor of SM quarks and leptons, where the bars are simply notations and do not mean the Dirac conjugation. Hypercharges are given by $\{Y_{Q_L} = Y_{u_L} = Y_{d_L}, Y_{u_R^\dagger}, Y_{d_R^\dagger}, Y_{L_L} = Y_{e_L} = Y_\nu, Y_{e_R^\dagger}\} = \{1/6, -2/3, 1/3, -1/2, 1\}$. After integrating out sfermions with mass $M_{\tilde{f}}$ in the right panel of Fig. 1, we obtain dim-6 operators between the SM fermion pair and \tilde{B} pair,

$$\mathcal{L}_{\text{eff}} = \sum_{f=q,l} \frac{(\sqrt{2}g_1 Y_f)(\sqrt{2}g_1 Y_f)}{M_{\tilde{f}}^2} (f^\dagger \tilde{B}^\dagger)(f \tilde{B}), \tag{C1}$$

where for simplicity we consider a universal mass for all the fermions, i.e., $M_{\tilde{f}} \equiv M_{\tilde{q}} = M_{\tilde{l}}$.

The amplitude squared terms in the collision term for the $f\bar{f} \rightarrow \tilde{B} \tilde{B}$ scattering process is given by⁶

$$\begin{aligned}
\sum_{\text{internal d.o.f.}} \int d\Omega |\mathcal{M}|_{f\bar{f} \rightarrow \tilde{B} \tilde{B}}^2 &\approx 2\pi N_{\text{flavor}} \left[N_{\text{color}} \left(\sum_{i,j=1}^2 (\delta_i^j)^2 Y_{Q_L}^4 + Y_{u_R^\dagger}^4 + Y_{d_R^\dagger}^4 \right) + \left(\sum_{i,j=1}^2 (\delta_i^j)^2 Y_{L_L}^4 + Y_{e_R^\dagger}^4 \right) \right] \left(\frac{g_1^2}{M_{\tilde{f}}^2} \right)^2 \left[\frac{16}{3} s^2 \right] \\
&= \frac{1520\pi}{27} \frac{g_1^4}{M_{\tilde{f}}^4} s^2,
\end{aligned} \tag{C2}$$

where $N_{\text{flavor}} = N_{\text{color}} = 3$. As in Eq. (B2), if we neglect bino mass, then the collision term can be approximately given by [using $\int_0^\infty dx x^6 K_1(x) = 384$]

$$\begin{aligned}
C_{f\bar{f} \rightarrow \tilde{B} \tilde{B}} &\approx \frac{T}{2048\pi^6} \int_{4M_1^2}^{\infty} ds (s - 4M_1^2)^{1/2} K_1(\sqrt{s}/T) \sum_{\text{internal d.o.f.}} \int d\Omega |\mathcal{M}|_{f\bar{f} \rightarrow \tilde{B} \tilde{B}}^2 \\
&\approx \frac{T}{2048\pi^6} \left(\frac{1520\pi}{27} \frac{g_1^4}{M_{\tilde{f}}^4} \right) \int_{4M_1^2}^{\infty} ds s^{5/2} K_1(\sqrt{s}/T) \\
&\approx \frac{T}{2048\pi^6} \left(\frac{1520\pi}{27} \frac{g_1^4}{M_{\tilde{f}}^4} \right) \int_0^\infty (Tdx)(2Tx)(xT)^5 K_1(x) \\
&= \frac{190}{9} g_1^4 \frac{1}{\pi^5} \frac{1}{M_{\tilde{f}}^4} T^8.
\end{aligned} \tag{C3}$$

APPENDIX D: THE CALCULATION DETAILS IN CASE III A

When neglecting all particle masses in the final state, we have

$$\begin{aligned}
\sum_{\text{internal d.o.f.}} \int d\Omega |\mathcal{M}|_{HH^* \rightarrow \tilde{B} \tilde{W}}^2 &\approx (2\pi) \times \left[\sum_{b=1}^3 \text{tr} \left(\frac{1}{2} \sigma^b \frac{1}{2} \sigma^b \right) \right] [Y_H^2] \left(\frac{g_1 g_2 \sin \beta \cos \beta}{\mu} \right)^2 [64s] \\
&= (48\pi) \times \frac{g_1^2 g_2^2}{\mu^2} \sin^2 \beta \cos^2 \beta s,
\end{aligned} \tag{D1}$$

⁶Again, fields in the initial and final states in the process should be understood in the sense of physical particles, where \bar{f} denotes the physical antiparticle. Discussion on the naming convention of particles, states, and fields can be found in, e.g., [42].

$$\begin{aligned}
\sum_{\text{internal d.o.f.}} \int d\Omega |\mathcal{M}|_{\tilde{W}H \rightarrow \tilde{B}H}^2 &= \sum_{\text{internal d.o.f.}} \int d\Omega |\mathcal{M}|_{\tilde{W}H^* \rightarrow \tilde{B}H^*}^2 \\
&\approx (2\pi) \times \left[\sum_{b=1}^3 \text{tr} \left(\frac{1}{2} \sigma^b \frac{1}{2} \sigma^b \right) \right] [Y_H^2] \left(\frac{g_1 g_2 \sin \beta \cos \beta}{\mu} \right)^2 [32s] \\
&= (24\pi) \times \frac{g_1^2 g_2^2}{\mu^2} \sin^2 \beta \cos^2 \beta s,
\end{aligned} \tag{D2}$$

$$\begin{aligned}
\sum_{\text{internal d.o.f.}} \int d\Omega |\mathcal{M}|_{\tilde{f}\tilde{f} \rightarrow \tilde{B}\tilde{W}}^2 &\approx 2\pi \left[\sum_{b=1}^3 \text{tr} \left(\frac{1}{2} \sigma^b \frac{1}{2} \sigma^b \right) \right] [N_{\text{flavor}} (Y_{L_L}^2 + N_{\text{color}} Y_{Q_L}^2)] \left(\frac{g_1 g_2}{M_{\tilde{f}}^2} \right)^2 \left[\frac{16}{3} s^2 \right] \\
&= (16\pi) \times \frac{g_1^2 g_2^2}{M_{\tilde{f}}^4} s^2,
\end{aligned} \tag{D3}$$

$$\begin{aligned}
\sum_{\text{internal d.o.f.}} \int d\Omega |\mathcal{M}|_{\tilde{W}f \rightarrow \tilde{B}f}^2 &= \sum_{\text{internal d.o.f.}} \int d\Omega |\mathcal{M}|_{\tilde{W}\tilde{f} \rightarrow \tilde{B}\tilde{f}}^2 \\
&\approx 2\pi \left[\sum_{b=1}^3 \text{tr} \left(\frac{1}{2} \sigma^b \frac{1}{2} \sigma^b \right) \right] [N_{\text{flavor}} (Y_{L_L}^2 + N_{\text{color}} Y_{Q_L}^2)] \left(\frac{g_1 g_2}{M_{\tilde{f}}^2} \right)^2 \left[\frac{32}{3} s^2 \right] \\
&= (32\pi) \times \frac{g_1^2 g_2^2}{M_{\tilde{f}}^4} s^2,
\end{aligned} \tag{D4}$$

$$\begin{aligned}
\sum_{\text{internal d.o.f.}} \int d\Omega |\mathcal{M}|_{\tilde{f}\tilde{f} \rightarrow \tilde{B}\tilde{G}}^2 &\approx 2\pi \left[\sum_{a=1}^8 \text{tr} \left(\frac{1}{2} \lambda^a \frac{1}{2} \lambda^a \right) \right] \left[N_{\text{flavor}} \left(\sum_{i,j=1}^2 (\delta_i^j)^2 Y_{Q_L}^2 + Y_{u_R}^2 + Y_{d_R}^2 \right) \right] \left(\frac{g_1 g_3}{M_{\tilde{f}}^2} \right)^2 \left[\frac{16}{3} s^2 \right] \\
&= \left(\frac{704\pi}{9} \right) \times \frac{g_1^2 g_3^2}{M_{\tilde{f}}^4} s^2,
\end{aligned} \tag{D5}$$

$$\begin{aligned}
\sum_{\text{internal d.o.f.}} \int d\Omega |\mathcal{M}|_{\tilde{G}f \rightarrow \tilde{B}f}^2 &= \sum_{\text{internal d.o.f.}} \int d\Omega |\mathcal{M}|_{\tilde{G}\tilde{f} \rightarrow \tilde{B}\tilde{f}}^2 \\
&\approx 2\pi \left[\sum_{a=1}^8 \text{tr} \left(\frac{1}{2} \lambda^a \frac{1}{2} \lambda^a \right) \right] \left[N_{\text{flavor}} \left(\sum_{i,j=1}^2 (\delta_i^j)^2 Y_{Q_L}^2 + Y_{u_R}^2 + Y_{d_R}^2 \right) \right] \left(\frac{g_1 g_3}{M_{\tilde{f}}^2} \right)^2 \left[\frac{32}{3} s^2 \right] \\
&= \left(\frac{1408\pi}{9} \right) \times \frac{g_1^2 g_3^2}{M_{\tilde{f}}^4} s^2.
\end{aligned} \tag{D6}$$

APPENDIX E: THE CALCULATION DETAILS IN CASE III B

The $1 \rightarrow 3$ decay processes are indicated by the red colored arrow in Fig. 1. When neglecting all particle masses in the final state, we have

$$\begin{aligned}
\Gamma_{\tilde{W} \rightarrow \tilde{B}HH^*} &= \frac{1}{(2\pi)^3} \frac{1}{32M_2^3} \frac{1}{g_{\tilde{W}}} \sum_{\text{internal d.o.f.}} \int dm_{12}^2 dm_{23}^2 |\mathcal{M}|_{\tilde{W} \rightarrow \tilde{B}HH^*}^2 \\
&= \frac{1}{(2\pi)^3} \frac{1}{32M_2^3} \frac{1}{\sum_{b=1}^3 (2s_{\tilde{W}} + 1)} \left[\sum_{b=1}^3 \text{tr} \left(\frac{1}{2} \sigma^b \frac{1}{2} \sigma^b \right) \right] [Y_H^2] \left[\frac{32}{3} M_2^6 \left(\frac{g_1 g_2 \sin \beta \cos \beta}{\mu} \right)^2 \right] \\
&= \frac{1}{384\pi^3} \left(\frac{g_1 g_2 \sin \beta \cos \beta}{\mu} \right)^2 M_2^3,
\end{aligned} \tag{E1}$$

$$\begin{aligned}
\Gamma_{\tilde{W} \rightarrow \tilde{B} f \bar{f}} &= \frac{1}{(2\pi)^3} \frac{1}{32M_2^3} \frac{1}{g_{\tilde{W}}} \sum_{\text{internal d.o.f.}} \int dm_{12}^2 dm_{23}^2 |\mathcal{M}|_{\tilde{W} \rightarrow \tilde{B} f \bar{f}}^2 \\
&= \frac{1}{(2\pi)^3} \frac{1}{32M_2^3} \frac{1}{\sum_{b=1}^3 (2s_{\tilde{W}} + 1)} \left[\sum_{b=1}^3 \text{tr} \left(\frac{1}{2} \sigma^b \frac{1}{2} \sigma^b \right) \right] [N_{\text{flavor}} (Y_{L_L}^2 + N_{\text{color}} Y_{Q_L}^2)] \left[\frac{2}{3} M_2^8 \left(\frac{g_1 g_2}{M_f^2} \right)^2 \right] \\
&= \frac{1}{1536\pi^3} \left(\frac{g_1 g_2}{M_f^2} \right)^2 M_2^5,
\end{aligned} \tag{E2}$$

$$\begin{aligned}
\Gamma_{\tilde{G} \rightarrow \tilde{B} f \bar{f}} &= \frac{1}{(2\pi)^3} \frac{1}{32M_3^3} \frac{1}{g_{\tilde{G}}} \sum_{\text{internal d.o.f.}} \int dm_{12}^2 dm_{23}^2 |\mathcal{M}|_{\tilde{G} \rightarrow \tilde{B} f \bar{f}}^2 \\
&= \frac{1}{(2\pi)^3} \frac{1}{32M_3^3} \frac{1}{\sum_{a=1}^8 (2s_{\tilde{G}} + 1)} \left[\sum_{a=1}^8 \text{tr} \left(\frac{1}{2} \lambda^a \frac{1}{2} \lambda^a \right) \right] \left[N_{\text{flavor}} \left(\sum_{i,j=1}^2 (\delta_i^j)^2 Y_{Q_L}^2 + Y_{u_R}^2 + Y_{d_R}^2 \right) \right] \left[\frac{2}{3} M_2^8 \left(\frac{g_1 g_3}{M_f^2} \right)^2 \right] \\
&= \frac{11}{9216\pi^3} \left(\frac{g_1 g_3}{M_f^2} \right)^2 M_2^5,
\end{aligned} \tag{E3}$$

where dm_{12}^2, dm_{23}^2 are defined in [70].

APPENDIX F: THE CALCULATION DETAILS OF TWO-BODY DECAY AFTER EWSB

As discussed in Sec. IV A, we have the following $1 \rightarrow 2$ decay possibly affecting the cosmological BBN:

$$\begin{aligned}
\Gamma_{\tilde{\chi}_2^0 \rightarrow \tilde{\chi}_1^0 h} &= \frac{1}{2s_{\tilde{\chi}_2^0} + 1} \frac{1}{2M_2} \sum_{\text{spin d.o.f.}} \int d\Pi_2 |M|_{\tilde{\chi}_2^0 \rightarrow \tilde{\chi}_1^0 h}^2 \\
&= \frac{1}{2} \frac{1}{2M_2} \int d\Pi_2 \left(\frac{v}{\mu} g_1 g_2 \sin \beta \cos \beta \right)^2 \left[4 \left(p_{\tilde{\chi}_2^0} \cdot p_{\tilde{\chi}_1^0} + M_{\tilde{\chi}_2^0} M_{\tilde{\chi}_1^0} \right) \right] \\
&\approx \frac{1}{2} \frac{1}{2M_2} \left[\int d\Omega \frac{1}{16\pi^2} \frac{|\vec{p}_{\tilde{\chi}_1^0}|}{M_2} \right] \left(\frac{v}{\mu} g_1 g_2 \sin \beta \cos \beta \right)^2 \left[4(M_2 E_{\tilde{\chi}_1^0} + M_2 M_1) \right],
\end{aligned} \tag{F1}$$

where

$$E_{\tilde{\chi}_1^0} = \frac{M_2^2 + M_1^2 - M_h^2}{2M_2} \approx \frac{M_2^2 + M_1^2}{2M_2}, \tag{F2}$$

$$\begin{aligned}
|\vec{p}_{\tilde{\chi}_1^0}| &= \sqrt{E_{\tilde{\chi}_1^0}^2 - M_1^2} = \frac{(M_2^4 + M_1^4 + M_h^4 - 2M_2^2 M_1^2 - 2M_2^2 M_h^2 - 2M_1^2 M_h^2)^{\frac{1}{2}}}{2M_2} \\
&\approx \frac{M_2^2 - M_1^2}{2M_2}.
\end{aligned} \tag{F3}$$

Finally, we have [47]

$$\begin{aligned}
\Gamma_{\tilde{\chi}_2^0 \rightarrow \tilde{\chi}_1^0 h} &\approx \frac{1}{2} \frac{1}{2M_2} \left[4\pi \frac{1}{16\pi^2} \frac{1}{2} \left(1 - \frac{M_1^2}{M_2^2} \right) \right] \left(\frac{v}{\mu} g_1 g_2 \sin \beta \cos \beta \right)^2 \left[4M_2 \frac{(M_2 + M_1)^2}{2M_2} \right] \\
&\approx M_2 \frac{1}{16\pi} \left(\frac{v}{\mu} g_1 g_2 \sin \beta \cos \beta \right)^2 \left(1 - \frac{M_1^2}{M_2^2} \right) \left(1 + \frac{M_1}{M_2} \right)^2.
\end{aligned} \tag{F4}$$

Using the GET we would obtain the same results in the high-energy limit for $\Gamma_{\tilde{\chi}_1^\pm \rightarrow \tilde{\chi}_1^0 W^\pm}$.

- [1] Y. A. Golfand and E. P. Likhtman, Extension of the algebra of Poincaré group generators and violation of p invariance, *JETP Lett.* **13**, 323 (1971).
- [2] D. V. Volkov and V. P. Akulov, Is the neutrino a Goldstone particle?, *Phys. Lett.* **46B**, 109 (1973).
- [3] J. Wess and B. Zumino, Supergauge transformations in four dimensions, *Nucl. Phys.* **B70**, 39 (1974).
- [4] A. Salam and J. Strathdee, Super-symmetry and non-Abelian gauges, *Phys. Lett.* **51B**, 353 (1974).
- [5] J. Wess and B. Zumino, Supergauge invariant extension of quantum electrodynamics, *Nucl. Phys.* **B78**, 1 (1974).
- [6] S. Ferrara and B. Zumino, Supergauge invariant Yang-Mills theories, *Nucl. Phys.* **B79**, 413 (1974).
- [7] G. Steigman and M. S. Turner, Cosmological constraints on the properties of weakly interacting massive particles, *Nucl. Phys.* **B253**, 375 (1985).
- [8] G. Jungman, M. Kamionkowski, and K. Griest, Super-symmetric dark matter, *Phys. Rep.* **267**, 195 (1995).
- [9] S. P. Martin, A supersymmetry primer, in *Advanced Series on Directions in High Energy Physics | Perspectives on Supersymmetry* (World Scientific, Singapore, 1998), pp. 1–98, 10.1142/9789812839657_0001.
- [10] J. L. Feng, Dark matter candidates from particle physics and methods of detection, *Annu. Rev. Astron. Astrophys.* **48**, 495 (2010).
- [11] J. Cao, C. Han, L. Wu, J. M. Yang, and Y. Zhang, Probing natural SUSY from stop pair production at the LHC, *J. High Energy Phys.* **11** (2012) 039.
- [12] J. Cao, F. Ding, C. Han, J. M. Yang, and J. Zhu, A light Higgs scalar in the NMSSM confronted with the latest LHC Higgs data, *J. High Energy Phys.* **11** (2013) 018.
- [13] C. Han, A. Kobakhidze, N. Liu, A. Saavedra, L. Wu, and J. M. Yang, Probing light Higgsinos in natural SUSY from monojet signals at the LHC, *J. High Energy Phys.* **02** (2014) 049.
- [14] C. Han, K.-i. Hikasa, L. Wu, J. M. Yang, and Y. Zhang, Current experimental bounds on stop mass in natural SUSY, *J. High Energy Phys.* **10** (2013) 216.
- [15] C. Han, D. Kim, S. Munir, and M. Park, Accessing the core of naturalness, nearly degenerate Higgsinos, at the LHC, *J. High Energy Phys.* **04** (2015) 132.
- [16] C. Han, J. Ren, L. Wu, J. M. Yang, and M. Zhang, Top-squark in natural SUSY under current LHC run-2 data, *Eur. Phys. J. C* **77**, 93 (2017).
- [17] C. Han, K.-i. Hikasa, L. Wu, J. M. Yang, and Y. Zhang, Status of CMSSM in light of current LHC run-2 and LUX data, *Phys. Lett. B* **769**, 470 (2017).
- [18] ATLAS Collaboration, SUSY March 2023 summary plot update, <https://cds.cern.ch/record/2852738>.
- [19] CMS Collaboration, CMS SUS physics results, <https://twiki.cern.ch/twiki/bin/view/CMSPublic/PhysicsResultsSUS>.
- [20] H. Baer, V. Barger, S. Salam, D. Sengupta, and K. Sinha, Status of weak scale supersymmetry after LHC run 2 and ton-scale noble liquid WIMP searches, *Eur. Phys. J. Special Topics* **229**, 3085 (2020).
- [21] F. Wang, W. Wang, J. Yang, Y. Zhang, and B. Zhu, Low energy supersymmetry confronted with current experiments: An overview, *Universe* **8**, 178 (2022).
- [22] J. M. Yang, P. Zhu, and R. Zhu, A brief survey of low energy supersymmetry under current experiments, *Proc. Sci. LHCP2022* (2022) 069.
- [23] G. Giudice and A. Romanino, Split supersymmetry, *Nucl. Phys.* **B699**, 65 (2004).
- [24] N. Arkani-Hamed, S. Dimopoulos, G. Giudice, and A. Romanino, Aspects of split supersymmetry, *Nucl. Phys.* **B709**, 3 (2005).
- [25] N. Arkani-Hamed and S. Dimopoulos, Supersymmetric unification without low energy supersymmetry and signatures for fine-tuning at the LHC, *J. High Energy Phys.* **06** (2005) 073.
- [26] J. D. Wells, PeV-scale supersymmetry, *Phys. Rev. D* **71**, 015013 (2005).
- [27] L. J. Hall and Y. Nomura, A finely-predicted Higgs boson mass from a finely-tuned weak scale, *J. High Energy Phys.* **03** (2010) 076.
- [28] G. F. Giudice and A. Strumia, Probing high-scale and split supersymmetry with Higgs mass measurements, *Nucl. Phys.* **B858**, 63 (2012).
- [29] M. Ibe, S. Matsumoto, and T. T. Yanagida, Pure gravity mediation with $m_{3/2} = 10\text{--}100$ TeV, *Phys. Rev. D* **85**, 095011 (2012).
- [30] L. E. Ibanez and I. Valenzuela, The Higgs mass as a signature of heavy SUSY, *J. High Energy Phys.* **05** (2013) 064.
- [31] L. J. Hall, Y. Nomura, and S. Shirai, Grand unification, axion, and inflation in intermediate scale supersymmetry, *J. High Energy Phys.* **06** (2014) 137.
- [32] S. A. R. Ellis and J. D. Wells, High-scale supersymmetry, the Higgs boson mass, and gauge unification, *Phys. Rev. D* **96**, 055024 (2017).
- [33] C. Liu, A supersymmetry model of leptons, *Phys. Lett. B* **609**, 111 (2005).
- [34] C. Liu, Supersymmetry for fermion masses, *Commun. Theor. Phys.* **47**, 1088 (2007).
- [35] H. Abe *et al.* (MAGIC Collaboration), Search for gamma-ray spectral lines from dark matter annihilation up to 100 TeV toward the Galactic Center with MAGIC, *Phys. Rev. Lett.* **130**, 061002 (2023).
- [36] E. W. Kolb and M. S. Turner, *The Early Universe* (CRC Press, Boca Raton, 1990), Vol. 69, 10.1201/9780429492860.
- [37] K. A. Olive and M. Srednicki, New limits on parameters of the supersymmetric standard model from cosmology, *Phys. Lett. B* **230**, 78 (1989).
- [38] K. Griest, M. Kamionkowski, and M. S. Turner, Super-symmetric dark matter above the W mass, *Phys. Rev. D* **41**, 3565 (1990).
- [39] L. J. Hall, K. Jedamzik, J. March-Russell, and S. M. West, Freeze-in production of FIMP dark matter, *J. High Energy Phys.* **03** (2010) 080.
- [40] G. Aad *et al.* (ATLAS Collaboration), Observation of a new particle in the search for the Standard Model Higgs boson with the ATLAS detector at the LHC, *Phys. Lett. B* **716**, 1 (2012).
- [41] S. Chatrchyan *et al.* (CMS Collaboration), Observation of a new boson at a mass of 125 GeV with the CMS experiment at the LHC, *Phys. Lett. B* **716**, 30 (2012).
- [42] H. K. Dreiner, H. E. Haber, and S. P. Martin, Two-component spinor techniques and Feynman rules for quantum field theory and supersymmetry, *Phys. Rep.* **494**, 1 (2010).
- [43] F. Elahi, C. Kolda, and J. Unwin, Ultraviolet freeze-in, *J. High Energy Phys.* **03** (2015) 048.

- [44] M. Beneke, R. Szafron, and K. Urban, Sommerfeld-corrected relic abundance of wino dark matter with NLO electroweak potentials, *J. High Energy Phys.* **02** (2021) 020.
- [45] J. Ikemoto, N. Haba, S. Yasuhiro, and T. Yamada, Higgs portal Majorana fermionic dark matter with the freeze-in mechanism, *Prog. Theor. Exp. Phys.* **2023**, 083B04 (2023).
- [46] A. Arvanitaki, C. Davis, P. W. Graham, A. Pierce, and J. G. Wacker, Limits on split supersymmetry from gluino cosmology, *Phys. Rev. D* **72**, 075011 (2005).
- [47] J. F. Gunion and H. E. Haber, Two-body decays of neutralinos and charginos, *Phys. Rev. D* **37**, 2515 (1988).
- [48] J. F. Gunion and H. E. Haber, Errata for Higgs bosons in supersymmetric models: 1, 2, and 3, arXiv:hep-ph/9301205.
- [49] A. Djouadi, Y. Mambrini, and M. Muhlleitner, Chargino and neutralino decays revisited, *Eur. Phys. J. C* **20**, 563 (2001).
- [50] Y. Yamada, Electroweak two-loop contribution to the mass splitting within a new heavy SU(2)(L) fermion multiplet, *Phys. Lett. B* **682**, 435 (2010).
- [51] M. Ibe, S. Matsumoto, and R. Sato, Mass splitting between charged and neutral winos at two-loop level, *Phys. Lett. B* **721**, 252 (2013).
- [52] J. McKay and P. Scott, Two-loop mass splittings in electroweak multiplets: Winos and minimal dark matter, *Phys. Rev. D* **97**, 055049 (2018).
- [53] M. Ibe, M. Mishima, Y. Nakayama, and S. Shirai, Precise estimate of charged wino decay rate, *J. High Energy Phys.* **01** (2023) 017.
- [54] M. Kawasaki, K. Kohri, T. Moroi, and A. Yotsuyanagi, Big-bang nucleosynthesis and gravitino, *Phys. Rev. D* **78**, 065011 (2008).
- [55] M. Kawasaki, K. Kohri, T. Moroi, and Y. Takaesu, Revisiting big-bang nucleosynthesis constraints on long-lived decaying particles, *Phys. Rev. D* **97**, 023502 (2018).
- [56] K. Rolbiecki and K. Sakurai, Long-lived bino and wino in supersymmetry with heavy scalars and Higgsinos, *J. High Energy Phys.* **11** (2015) 091.
- [57] G. Aad *et al.* (ATLAS Collaboration), Search for neutral long-lived particles in pp collisions at $\sqrt{s} = 13$ TeV that decay into displaced hadronic jets in the ATLAS calorimeter, *J. High Energy Phys.* **06** (2022) 005.
- [58] A. Tumasyan *et al.* (CMS Collaboration), Search for long-lived particles decaying to a pair of muons in proton-proton collisions at $\sqrt{s} = 13$ TeV, *J. High Energy Phys.* **05** (2023) 228.
- [59] G. Aad *et al.* (ATLAS Collaboration), Search for long-lived charginos based on a disappearing-track signature using 136 fb^{-1} of pp collisions at $\sqrt{s} = 13$ TeV with the ATLAS detector, *Eur. Phys. J. C* **82**, 606 (2022).
- [60] A. M. Sirunyan *et al.* (CMS Collaboration), Search for disappearing tracks in proton-proton collisions at $\sqrt{s} = 13$ TeV, *Phys. Lett. B* **806**, 135502 (2020).
- [61] S. P. Martin, Nonuniversal gaugino masses from nonsinglet F -terms in nonminimal unified models, *Phys. Rev. D* **79**, 095019 (2009).
- [62] S. P. Martin, Nonuniversal gaugino masses and seminatural supersymmetry in view of the Higgs boson discovery, *Phys. Rev. D* **89**, 035011 (2014).
- [63] S. Raza, Q. Shafi, and C. S. Un, $b - \tau$ Yukawa unification in SUSY SU(5) with mirage mediation: LHC and dark matter implications, *J. High Energy Phys.* **05** (2019) 046.
- [64] J. Edsjo and P. Gondolo, Neutralino relic density including coannihilations, *Phys. Rev. D* **56**, 1879 (1997).
- [65] N. D. Christensen and C. Duhr, FeynRules—Feynman rules made easy, *Comput. Phys. Commun.* **180**, 1614 (2009).
- [66] A. Alloul, N. D. Christensen, C. Degrande, C. Duhr, and B. Fuks, FeynRules 2.0—A complete toolbox for tree-level phenomenology, *Comput. Phys. Commun.* **185**, 2250 (2014).
- [67] T. Hahn, Generating Feynman diagrams and amplitudes with FeynArts 3, *Comput. Phys. Commun.* **140**, 418 (2001).
- [68] V. Shtabovenko, R. Mertig, and F. Orellana, New developments in FeynCalc 9.0, *Comput. Phys. Commun.* **207**, 432 (2016).
- [69] P. Gondolo and G. Gelmini, Cosmic abundances of stable particles: Improved analysis, *Nucl. Phys.* **B360**, 145 (1991).
- [70] R. L. Workman *et al.* (Particle Data Group Collaboration), Review of particle physics, *Prog. Theor. Exp. Phys.* **2022**, 083C01 (2022).